

# Frizzled-2 small interfering RNA protects hepatic BRL-3A cells against Hypoxia / Reoxygenation via modulation of autophagy

Xiang Hu<sup>1,2</sup> , Chenjie Zhou<sup>1</sup> , Guolin He<sup>1</sup> , Yuan Cheng<sup>1</sup> , MingXin Pan<sup>1</sup> , Yi Gao<sup>1</sup> 

<sup>1</sup>Department of Hepatobiliary Surgery II, State Key Laboratory of Organ Failure Research, Guangdong Provincial Research Center for Artificial Organ and Tissue Engineering, Guangzhou Clinical Research and Transformation Center for Artificial Liver, Institute of Regenerative Medicine, Zhujiang Hospital, Southern Medical University, Guangzhou, China

<sup>2</sup>Department of General Surgery, The Second Hospital of Shenzhen Baoan People's Hospital Group, Shenzhen, China

**Cite this article as:** Hu X, Zhou C, He G, Cheng Y, Pan M, Gao Y. Frizzled-2 small interfering RNA protects hepatic BRL-3A cells against Hypoxia / Reoxygenation via modulation of autophagy. *Turk J Gastroenterol* 2020; 31(2): 167-79.

## ABSTRACT

**Background/Aims:** Autophagy plays a positive role in the prevention of liver damage after hepatic ischemia-reperfusion injury (HIRI); however, the molecular mechanism is still a mystery. Understanding the molecular events behind this injury may have important implications for devising proper strategies for managing liver injury. This study investigated the effects of Frizzled-2 expression on autophagy as well as  $Ca^{2+}$  concentration and apoptosis in BRL-3A cells.

**Materials and Methods:** BRL-3A cells exposed to the hypoxia/reoxygenation (H/R) condition were used as an in vitro HIRI hepatic cell model. The transfection of Frizzled-2 small interfering RNA (siRNA) or expression vector was performed to silence or overexpress Frizzled-2 in BRL-3A cells. The intracellular  $Ca^{2+}$  concentration was monitored by the fluorescence of  $Ca^{2+}$ . Western blot was used to detect autophagy-related proteins and apoptotic marker Caspase-3. The cellular autophagosome was observed by a transmission electron microscope.

**Results:** Beclin-1 and Atg7 expressions were considerably induced by H/R treatment, and this induction was attenuated by Frizzled-2 siRNA in BRL-3A cells. The LC3B-II/I ratio was inhibited by H/R treatment, although it was considerably induced by Frizzled-2 siRNA. The overexpression of Frizzled-2 induced intracellular  $Ca^{2+}$  concentration and expressed autophagy-related proteins and Caspase-3 except for the suppression of LC3B-II/I ratio in BRL-3A cells in the normoxia condition.

**Conclusion:** The overexpression of Frizzled-2 mimicked H/R treatment and suppressed autophagy activity, whereas Frizzled-2 siRNA induced cellular autophagy and attenuated the H/R-induced hepatic injury in BRL-3A cells. These developments suggest that Frizzled-2 siRNA protects hepatic BRL-3A cells from the injury of H/R via autophagy modulation.

**Keywords:** Frizzled-2, Hypoxia/Reoxygenation, autophagy, frizzled-2 siRNA, apoptosis, transmission electron microscopy

## INTRODUCTION

Hepatic ischemia-reperfusion injury (HIRI) is a major cause of liver injury in numerous clinical conditions, including liver surgery (1, 2), liver transplantation (3, 4), and hepatocellular carcinomas (5). In response to various types of stress or injury, autophagy activation plays an important role in programmed cell death and cellular self-protection. Autophagy is a complicated cellular process and is considered an adaptive response to stress. During the autophagy process, damaged proteins and organelles are degraded and recycled via lysosomal degradation, including three different major pathways: chaperone-mediated autophagy, microautophagy, and macroautophagy (6, 7). Among the three, macroautophagy has been extensively studied in mammals and is referred to as "autophagy." In this pathway, a double-membrane structure, known as "autophagosome," is formed with a portion of cytoplasm surrounded by

an isolation membrane or phagophore. A compartment, known as "autolysosome," is formed when the double-membrane autophagosome fuses with the lysosome, which results in the cellular degradation of autophagosomal contents by lysosomal enzymes (8). Autophagy is involved in the selective degrading of single, soluble proteins; it also prevents the accumulation of damaged and dysfunctional constituents and organelles in cells. By reorganizing cytoplasmic proteins and organelles and modulating intracellular energy, autophagy provides essential machinery for liver regeneration and mitotic or hypertrophic hepatocytes under HIRI stress. The activation of autophagy may be one of the mechanisms that can be used to alleviate liver HIRI. Autophagy-related proteins, including Atg7, Beclin-1, and Microtubule-associated protein 1 light chain 3 (LC3), are involved in autophagy activation and serve as markers of autophagy activity during injury (9).

Corresponding Author: Yi Gao; [drgaoy@126.com](mailto:drgaoy@126.com)

Received: August 13, 2018 Accepted: February 14, 2019

© Copyright 2020 by The Turkish Society of Gastroenterology · Available online at [www.turkjgastroenterol.org](http://www.turkjgastroenterol.org)

DOI: 10.5152/tjg.2020.18507

The accumulation of intracellular  $\text{Ca}^{2+}$  has been shown to trigger the activation of adenosine monophosphate (AMP)-activated protein kinase (AMPK) and the mammalian target of rapamycin (mTOR), which are crucial signaling pathways in regulating autophagy (10). Frizzled-2 plays an important role in driving the epithelial-mesenchymal transition through non-canonical Wnt5a/Frizzled-2 signaling in hepatocellular carcinoma (HCC) and liver regeneration by impacting hepatocyte proliferation, invasiveness, and metastasis; moreover, Frizzled-2 overexpression has been correlated with poor patient survival (1-3). We recently showed that Frizzled-2 expression was induced in BRL-3A cells with hypoxia/reoxygenation (H/R) treatment as well as in liver tissues in *in vivo* mice under IRI. The upregulation of the Frizzled-2/Wnt5a pathway was correlated with an increase in Caspase-3 dependent apoptosis accompanied by an overload of intracellular  $\text{Ca}^{2+}$  concentration and a decrease in  $\beta$ -catenin signaling in BRL-3A cells upon H/R treatment (11). However, the involvement of autophagy in the role of the Frizzled-2/Wnt5a pathway during the H/R-induced hepatic injury remained a mystery. Given the role of autophagy in dealing with stress, we hypothesize that Frizzled-2 could be involved in regulating autophagy activity in response to the H/R challenge.

This study investigated the role of Frizzled-2 in regulating autophagy and apoptosis using the H/R-induced rat normal liver BRL-3A cells—an *in vitro* cell model established to mimic the pathophysiological HIRI (11). We examined the effects of Frizzled-2 gene expression on the intracellular  $\text{Ca}^{2+}$  level, the expression of autophagy-related proteins (e.g., Beclin-1, Atg7, LC3B-I, and LC3B-II), and apoptosis marker Caspase-3 in BRL-3A cells subjected to the transfection of Frizzled-2 siRNA or Frizzled-2 expression vector to silence or overexpress Frizzled-2 expression. The effects of Frizzled-2 expression on the number of autophagosomes were analyzed by a transmission electron microscope.

## MATERIALS AND METHODS

### BRL-3A cell H/R model and experimental groups

This study was approved by the Ethical Committee guide of Zhujiang Hospital and Southern Medical University for the care and use of laboratory animals (No. ZJYY-2016-GDEK-001). Rat hepatic tissue-derived BRL-3A cells (12) (American Type Culture Collection, Manassas, VA, USA) were maintained in Dulbecco's Modified Eagle's Medium (DMEM) containing 4.5 g/L glucose, 10% fetal bovine serum (FBS), and 1% penicillin/streptomycin. The cells were

incubated in a fresh medium for 24 h prior to H/R incubation. The H/R injury model was performed according to the previously described methods (11). The BRL-3A cells were exposed to hypoxia by placing the culture plates in a humidified incubation chamber thermoregulated at 37°C, with a gas mixture of 95%  $\text{N}_2$  and 5%  $\text{CO}_2$  for 4 h. Then, the cells were transferred to the second chamber containing 95% air and 5%  $\text{CO}_2$  for reoxygenation for 1 h. The cells were treated in different experimental groups: (1) the control cell group, in which BRL-3A cells were incubated in DMEM; (2) the cell H/R group, in which BRL-3A cells were treated under an anoxic condition for 4 h, followed by the reoxygenation condition for 1 h; (3) the NC-H/R group, and (4) the Si-H/R group, in which BRL-3A cells challenged with H/R were subjected to a transfection of negative control (NC) or Frizzled-2 siRNA at 50 nM; and (5) the FRI group, in which Frizzled-2 overexpression was transfected with Frizzled-2 expression vector in BRL-3A cells without H/R treatment.

### Transfection with Frizzled-2 small interfering RNA (siRNA)

The BRL-3A cells were plated in 6-well plates at a density of  $10^5$  cells/well or in 100 mm dishes with  $10^6$  cells in a growth medium without antibiotics. After cell growth reached 50%-60% confluence, transfection was performed using Lipofectamine 2000 from Invitrogen (ThermoFisher Scientific, MA, USA). The cells were incubated in Opti-MEM I Reduced Serum Medium from Invitrogen with and without Frizzled-2 siRNA-Lipofectamine 2000 complexes (50 nM) for 6 h and then with fresh DMEM with 10% FBS for 48 h. The transfection efficiency of siRNA was monitored by observing the fluorescence of cells transfected with FAM-labeled siRNA negative control (siRNA-NC) after 6 h. The cells were subsequently subjected to H/R treatment and harvested for other experiments. Three different non-overlapping siRNA duplexes and FAM-labeled siRNA-NC were designed and purchased from Sigma-Aldrich (Guangzhou, China). The sequences of Frizzled-2 siRNA and NC were as follows: 5'-GCUGUACUAUACUCUUAUdTdT-3' and 5'-UUCUCCGAACGUGUCACGUAUdTdT-3'.

### Construction of the Frizzled-2 cDNA expression vector

The full-length of Frizzled-2 complementary DNA (cDNA), which codes for the entire Frizzled-2 protein, was cloned by PCR amplification using cDNA library synthesized based on the rat heart tissue-derived RNA and ligation into pcDNA3.1+ expression vector (Dongsheng Biotech, Guangzhou, China). The amplification primers for subcloning were synthesized to contain restriction enzyme digestion recognition sites, as shown below: Friz-

zled-2-EcoRI (F): 5'-ccggaattcgccaccATGCGGGCCCG-CAGCGCCCTGCCC-3'; Frizzled-2-XhoI (R): 5'-ccgctc-gagTCACACGGTGGTCTCTCCATGCCGGCTG-3' (Jinweizhi Biotech, Suzhou, China). The subcloned Frizzled-2 cDNA construct (FRI) was confirmed by restriction enzyme digestion and DNA sequencing (Shenggong Biotech, Shanghai, China).

#### **Total RNA isolation and quantitative real-time PCR analysis**

Total RNA was isolated from BRL-3A cells using Trizol from Invitrogen (ThermoFisher Scientific, MA, USA), following the manufacturer's protocols. Quantitative real-time PCR (qRT-PCR) was performed using SYBR Green PCR SuperMix (ThermoFisher Scientific, MA, USA) in an ABI 7500 real-time PCR system (Applied Biosystems, Foster, CA, USA) with a thermal profile (95°C for 1 min, and 40 cycles of 95°C for 15 s; 55°C for 1 min for Frizzled-2 and 95°C for 1 min; and 40 cycles of 95°C for 15 s and 60°C for 1 min for Wnt5a and  $\beta$ -actin). The primer sequences of Frizzled-2, Wnt5a, and  $\beta$ -actin are listed below: Frizzled-2-F: 5'-TCGTTTTGCCGTCTCT-3', Frizzled-2-R: 5'-TAGCGGAATCGCTGCAT-3'; Wnt5a-F: 5'-CGTGGCTATGACCAGTTTAAG-3', Wnt5a-R: 5'-CCA-CAATCTCCGTGCACTT-3';  $\beta$ -actin-F: 5'-AGGGAAATC-GTGGCTGACAT-3',  $\beta$ -actin-R: 5'-GAACCGCTCATTGC-CGATAG-3'. The examined mRNA levels are presented relative to the average of all  $\Delta$ Ct-values in each sample using the cycle threshold (Ct) method after normalization to corresponding  $\beta$ -actin expression.

#### **Protein expression analysis by Western blot**

Total proteins were extracted from the BRL-3A cells using ice-cold radioimmunoprecipitation assay (RIPA) lysis and extraction buffer (10 mM Tris, 100 mM NaCl, 1 mM EDTA, 1 mM EGTA, 1 mM NaF, 20 mM  $\text{Na}_4\text{P}_2\text{O}_7$ , 2 mM  $\text{Na}_3\text{VO}_4$ , 0.1% sodium dodecyl sulfate (SDS), 0.5% sodium deoxycholate, 1% Triton-100, 10% glycerol, and 1 mM PMSF) containing 1  $\times$  cocktail of proteinase and phosphatase inhibitors (ThermoFisher Scientific, MA, USA). Protein concentrations were quantified using the BCA method (Beyotime Biotechnology Co. Ltd., Shanghai, China). Protein samples (20  $\mu$ g) were then subjected to SDS polyacrylamide gel electrophoresis (SDS-PAGE) using 12% resolving gel and 6% stacking gel. Electrophoresis was performed in the compression gel at 80 V for 20 min and, subsequently, in the separation gel at 120 V for 90 min. After separation in a polyacrylamide gel, protein transfer onto a PVDF membrane was performed via electroblotting (Millipore, Billerica, MA, USA). The membrane was blocked using 5% skim milk in TBST for 60 min at room temperature (18°C–22°C) and rinsed three

times with TBST for 10 min for each wash. Afterward, the blots were incubated overnight using specific primary antibodies Atg7, Beclin-1, LC3B-I, LC3B-II, Caspase-3 (Cell Signaling Technology, 1:1000 dilution) and GAPDH as a loading control (Cell Signaling Technology, 1:5000 dilution), followed by a wash three times with TBST for 10 min each and incubation with secondary antibodies (1:5000 dilution, Santa Cruz Biotechnology, CA, USA) at room temperature (18°C–22°C) for 90 min. The immunoreactive signal was developed using West-Q Pico ECL Solution (GenDEPOT, Barker, TX, USA). The integrated optical density of the bands was evaluated by Image-Pro Plus 6.0 software (Media Cybernetics Inc., Silver Spring, MD, USA). The levels of protein expression were relatively expressed as being normalized to GAPDH. Each experiment was repeated three times.

#### **Fluorescence of $\text{Ca}^{2+}$ and laser scanning confocal microscopy**

For calcium detection, cells were grown in 6-well plates and incubated with the intracellular  $\text{Ca}^{2+}$  indicator Fluo 8-AM from Invitrogen (ThermoFisher, MA, USA) at 37°C for 30 min, according to the manufacturer's protocols. The fluorescence intensity was monitored at 490 nm/515 nm (Ex/Em). Fluorescent images were taken by an LSM510 confocal laser scanning microscope (Carl Zeiss, Jena, Germany) and analyzed using Image-Pro Plus 6.0 software (Media Cybernetics, Silver Spring, MD, USA). The means of fluorescence density in cells were compared. Data were expressed and represented as the mean  $\pm$  SEM of integrated optical densities from at least three different experiments.

#### **Transmission electron microscopy (TEM)**

Autophagosomes, also known as "autophagic vacuoles," can be detected by TEM. Autophagic vacuoles have a double-membrane structure, which is partially visible as two parallel membrane bilayers with morphologically intact cytosol and/or organelles (9, 13). In this study, after a wash with 0.1 M cacodylate buffer (pH 7.4), the cells were first fixed in 2.5% glutaraldehyde in 0.1 M cacodylate buffer for 1 h and then in 1% osmium tetroxide buffer for post-fixation. After dehydration in a graded series of ethanol, the cells were embedded in an epoxy resin (Marivac Industries, Montreal, QC, Canada). Ultrathin (~70 nm) sections were cut and placed on the grids. The sections on the grids were double-contrast stained with uranyl acetate and lead citrate for electron microscopy (JEM-1230; JEOL, Tokyo, Japan). Images were viewed using a Hitachi 7600 TEM (Hitachi High-Technologies America, Inc., Schaumburg, IL, USA). In addition, the density of autophagic vacuoles was expressed by vacuoles/number of cells.

### Statistical analysis

All data are presented as the mean±standard error of the mean (SEM). One-way analysis of variance was used to examine the overall statistical differences using The Statistical Package for the Social Sciences (SPSS) software version 24.0 (IBM Corp.; Armonk, NY, USA). Differences between the groups were considered statistically significant at  $p<0.05$ .

## RESULTS

### Frizzled-2 siRNA induced autophagy in BRL-3A cells with H/R treatment

The inhibition of Wnt5a/Frizzled-2 pathways was achieved by inhibiting Frizzled-2 expression at both mRNA and protein levels via the transfection of Frizzled-2 siRNA (50 nM) (11). The effects of Frizzled-2 siRNA on the expressions of representative autophagy markers, including Beclin-1 and Atg7, were examined in BRL-3A cells with H/R treatment. The LC3B-II/I ratio, a hallmark of autophagy in mammalian cells, and the number of autophagic vacuoles were further analyzed to evaluate the role of Frizzled-2 signaling in regulating autophagic flux. Both Beclin-1 and Atg7 were considerably induced at the protein level by H/R treatment; the induction was attenuated by Frizzled-2 siRNA transfection (Figures 1a-c). The LC3B-II/I ratio was inhibited by H/R treatment but remarkably induced by Frizzled-2 siRNA (Figures 1a-d). These results suggest that H/R treatment impeded the autophagy activity due to the inhibited conversion of LC3B-I to LC3B-II, which could be reversed by Frizzled-2 siRNA. We further evaluated autophagic vacuoles using TEM. Substantial increases in both the number and size of nonfunctional vacuole vesicles were observed; however, compared with the normal control cell group (Figure 2a) by TEM image analysis, autophagosomes were not clearly shown in NC-H/R (Figure 2b) and H/R (Figure 2d) groups. The nonfunctional vacuole vesicles considerably decreased, whereas autophagosomes increased in the Si-H/R group with Frizzled-2 siRNA transfection (Figure 2c), compared with the normal control cell group (Figure 2a), NC-H/R group (Figure 2b), and H/R group (Figure 2d). These results indicate that Frizzled-2 siRNA transfection can induce the recovery of autophagy impaired by H/R treatment in BRL-3A cells.

### Frizzled-2/Wnt5a pathway was downregulated by Frizzled-2 siRNA in BRL-3A cells

To further determine the roles of the Wnt5a/Frizzled-2 pathway in cell autophagy in hepatic cells, the expression of Frizzled-2/Wnt5a was examined by overexpressing

the Frizzled-2 expression vector and silencing Frizzled-2 gene expression in BRL-3A cells via siRNA approach under normoxia. After the transfection of Frizzled-2 expression vector (FRI), the qPCR analysis showed the mRNA levels of Frizzled-2, followed by 266- and 3-fold increases in Wnt5a expression ( $p<0.01$ ; Figures 3a b), as compared with the control cell group. The protein expression of both Frizzled-2 and Wnt5a increased dramatically by 2.7- and 2.2-fold, as compared with the control cell group by Western blot assay (Figures 3c-e). On the contrary, the Frizzled-2 mRNA and protein expressions were suppressed by the transfection of Frizzled-2 siRNA, whereas the Wnt5a mRNA level remained unchanged, with a slight increase in the protein expression level compared with the NC group.

### Overexpression of Frizzled-2-induced accumulation of intracellular $Ca^{2+}$ in BRL-3A cells

To determine the role of activation of the Wnt5a/Frizzled-2 pathway in modulating the level of intracellular  $Ca^{2+}$ , confocal microscopy was used to examine the intensity of  $Ca^{2+}$  fluorescence of Fluo-3/AM after the transfection of Frizzled-2 expression vector or siRNA in BRL-3A cells. The  $Ca^{2+}$  fluorescence intensity considerably increased in the FRI group, compared with the control cell group ( $69.90\pm4.34$  vs.  $46.49\pm6.30$ ,  $p<0.05$ , Figures 4a, d, and e), whereas intensity was substantially inhibited in the Frizzled-2 siRNA group ( $23.71\pm7.68$  vs.  $46.99\pm6.32$ ,  $p<0.05$ , Figures 4b, c, and e).

### Frizzled-2 inhibited autophagy in hepatic BRL-3A cells under normoxia

To determine the role of Frizzled-2 in regulating autophagy activities and autophagic flux, BRL-3A cells were transfected with a Frizzled-2 expression vector or siRNA. Autophagy-related proteins and autophagosome markers LC3B-I and -II were detected by immunoblotting. Compared with the normal control cell group (Figures 5a-c, Atg7,  $1.00\pm0.00$  vs.  $1.95\pm0.08$ ,  $p<0.05$ ; Beclin-1,  $1.00\pm0.00$  vs.  $2.83\pm0.06$ ,  $p<0.05$ ), both Atg7 and Beclin-1 were considerably upregulated in the Frizzled-2 overexpressing cells. However, compared with the siRNA-NC group (Figures 5a-c, Atg7,  $1.00\pm0.00$  vs.  $0.48\pm0.03$ ,  $p<0.05$ ; Beclin-1,  $1.00\pm0.00$  vs.  $0.59\pm0.01$ ,  $p<0.05$ ), Atg7 and Beclin-1 were inhibited in cells transfected with Frizzled-2 siRNA. The LC3B-II level decreased while LC3B-I increased by Frizzled-2 overexpression (Figure 5a), leading to a substantial decrease in the LC3B-II/LC3B-I ratio (Figure 5d). This observation suggests that the conversion of LC3B-I to LC3B-II was blocked; it also suggests that the number of autophagosomes decreased and that

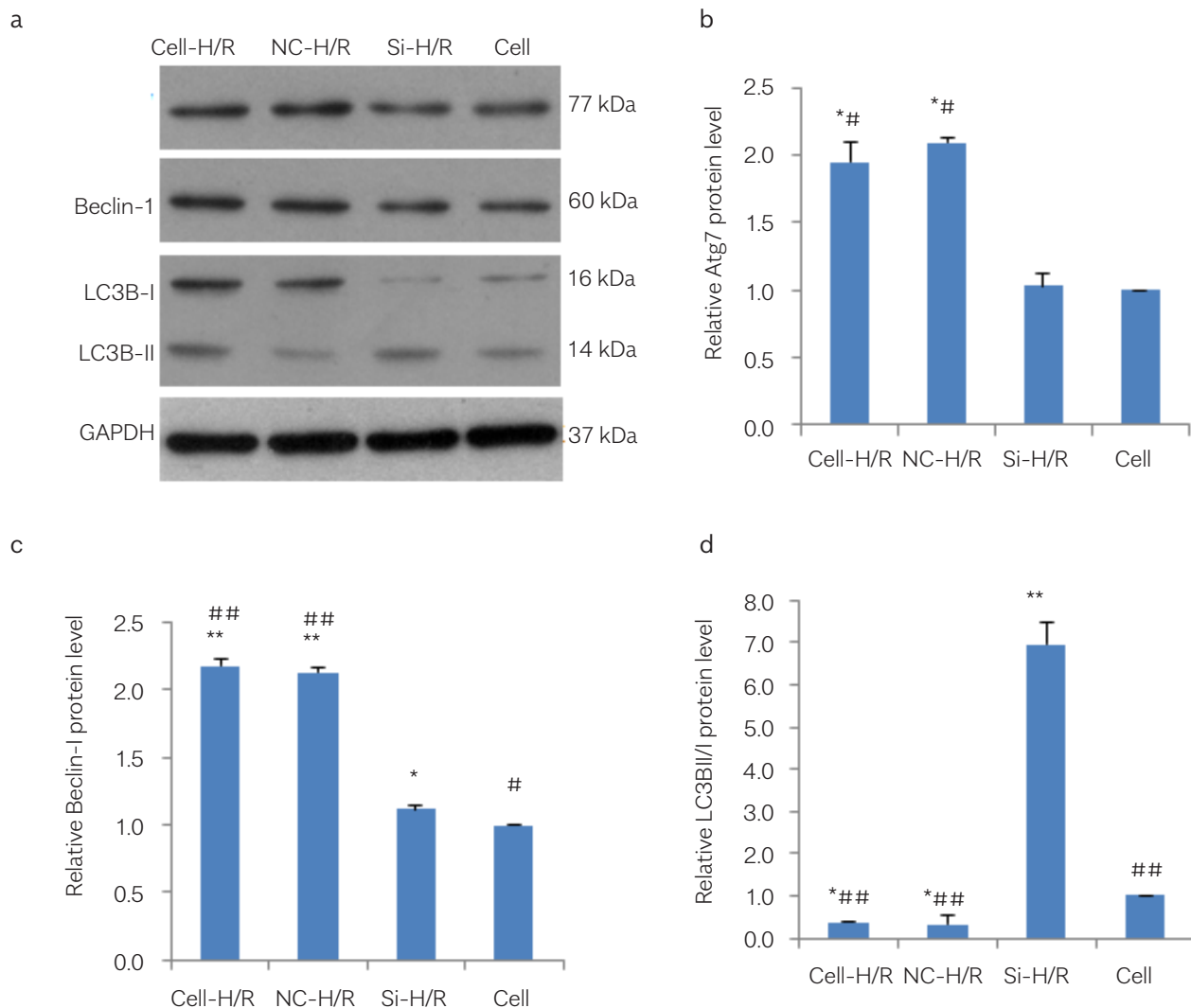


**Figure 1. a-d.** Effect of Frizzled-2 siRNA on the expressions of autophagy-related proteins in BRL-3A cells during H/R treatment. (a) Representative photographs of protein expression of Atg7, Beclin-1, LC3B-I/II, and GAPDH by immunoblotting; (b) Relative Atg7 protein expression. (c) Relative Beclin-1 expression; (d) The ratio of relative LC3B-I/II protein level. Band intensity was measured to quantify the relative protein expression and normalize it to GAPDH. Bar graphs are presented as means $\pm$ SEM from three independent experiments. \* $p < 0.05$  and \*\* $p < 0.001$  vs. cell group, and # $p < 0.05$  and ### $p < 0.001$  vs. Si-H/R group.

autophagic flux was inhibited by Frizzled-2 overexpression. Autophagosomes in transfected BRL-3A cells were further examined by electronic microscopy. The results showed fewer autophagosomes in the Frizzled-2-overexpressing BRL-3A cells than in the control cells (Figures 6a, d); they also indicated a higher number of autophagosomes in the Frizzled-2 siRNA transfected cells than in the siRNA-NC group (Figures 6b, c). These observations confirm that autophagy activity was inhibited by Frizzled-2 overexpression in BRL-3A cells under normoxia.

#### Frizzled-2-induced cell apoptosis in BRL-3A cells

Caspase-3, a crucial mediator of cell apoptosis, was examined to assess the effect of Frizzled-2 signaling on cell apoptosis in BRL-3A cells. The level of total Caspase-3 protein expression considerably increased by overexpressing Frizzled-2, compared with the control cell group ( $p < 0.001$ ). The total Caspase-3 protein expression was, however, suppressed by its siRNA transfection, compared with siRNA-NC ( $p < 0.05$ ) (Figures 7a, b), indicating that activated Frizzled-2 sig-



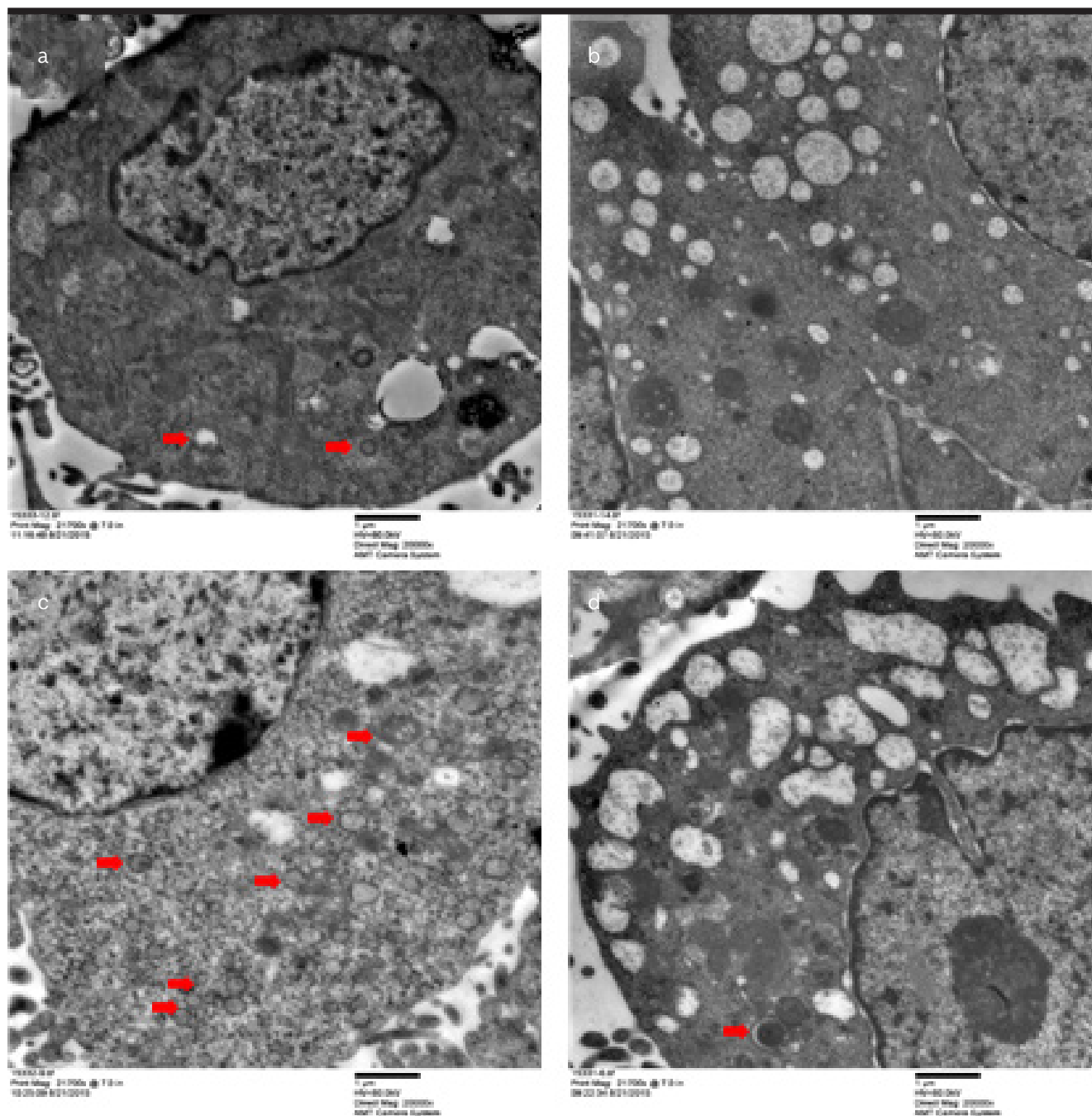


**Figure 2. a-d.** Frizzled-2 siRNA promoted autophagy flux in BRL-3A cells during H/R treatment. Representative TEM images showed autophagosomes or autophagic vacuoles (red arrows) in BRL-3A cells: (a) Cell group; (b) NC-H/R group; (c) Si-H/R; (d) H/R group. The numbers of autophagosomes (red arrows) were determined. Scale bars denote 1 µm.

naling may induce cell death. In contrast, the silence of Frizzled-2 gene expression may protect cells from apoptosis in hepatic BRL-3A cells.

## DISCUSSION

Autophagy has been shown to play a positive role in the prevention of liver damage after HIRI injury (14-17). In

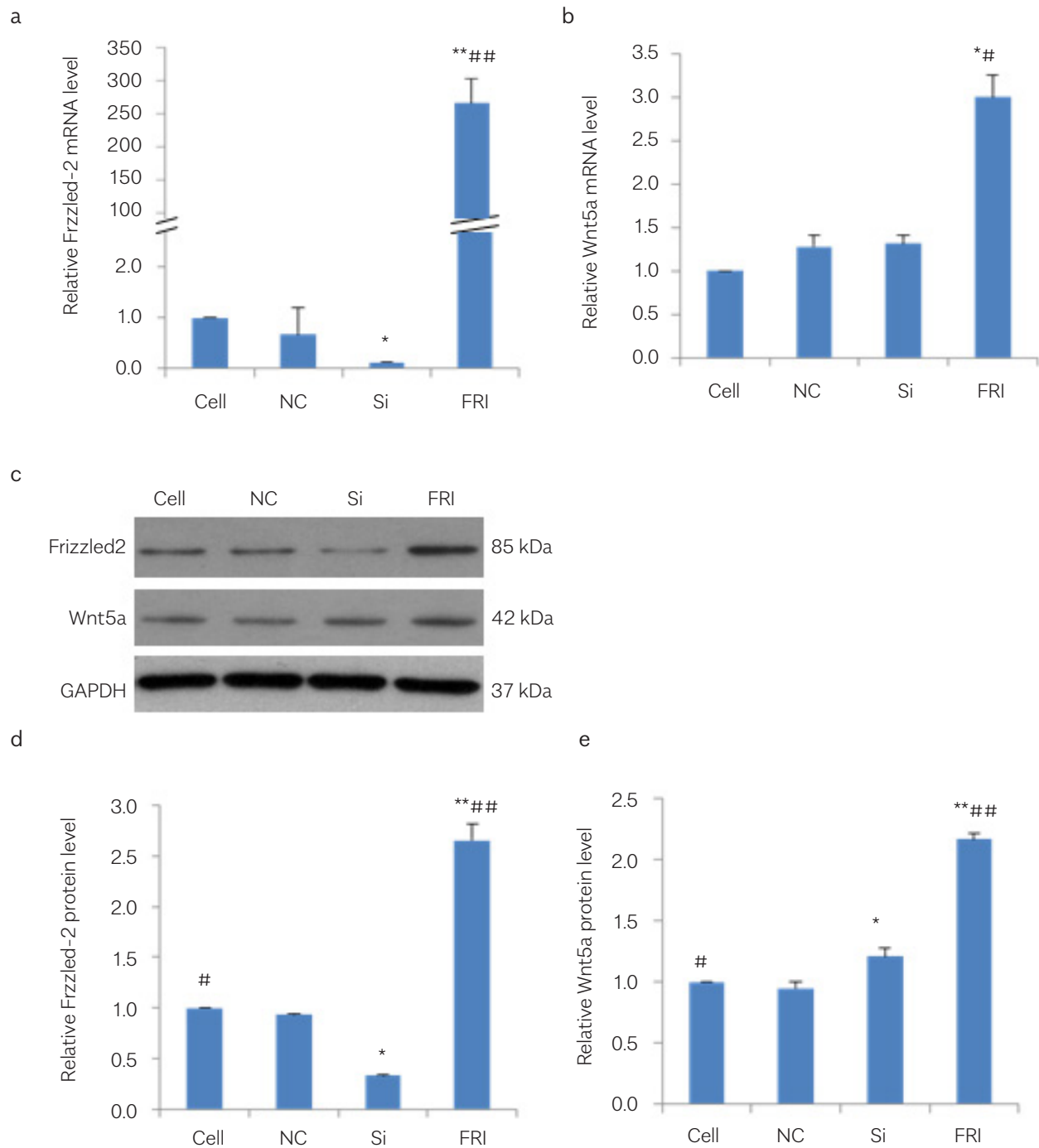


**Figure 3. a-e.** Expression of Frizzled-2 and Wnt5a at mRNA and protein levels in BRL-3A cells. The levels of mRNA and protein of Wnt5a and Frizzled-2 were detected using qPCR and Western blot, respectively. (a) The mRNA expression of the Frizzled-2 gene increased in cells transfected with Frizzled-2 plasmid (FRI) and downregulated in cells with Frizzled-2 siRNA transfection (Si). (b) Wnt5a mRNA expression was induced by Frizzled-2 overexpression (FRI). (c) Representative photographs of protein expression of Frizzled-2 and Wnt5a; (d) Relative Frizzled-2 protein expression level; (e) Relative Wnt5a protein expression level. The relative protein expression levels were expressed as band optical densities normalized to GAPDH expression. Data were presented as means±SEM from three independent experiments. \*p<0.05, \*\*p<0.001 vs. cell group; #p<0.05, ##p<0.001 vs. Si group.

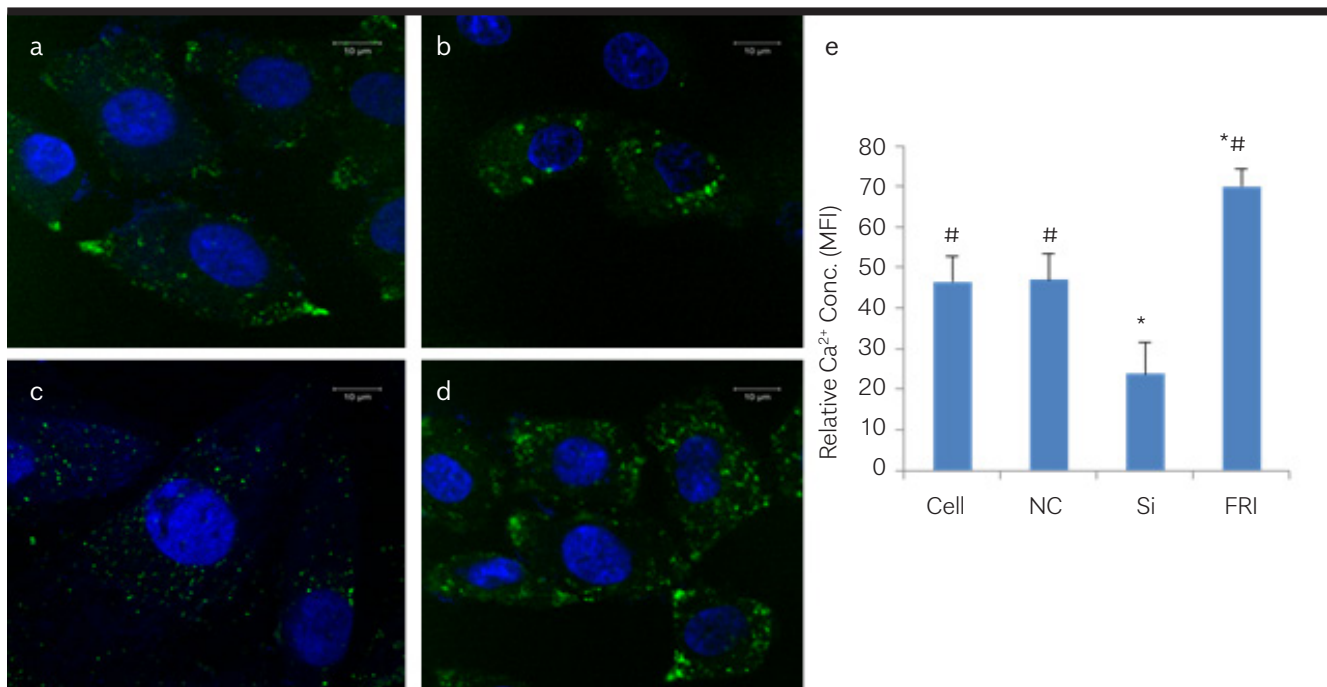


**Figure 4. a-e.** Frizzled-2 induced intracellular  $\text{Ca}^{2+}$  accumulation in BRL-3A cells. Fluorescence of intracellular  $\text{Ca}^{2+}$  denoted by Fluo-3/AM (green) was detected at 48 h following the transfection of Frizzled-2 plasmid or siRNA (50 nM); (a) Weak intensity of  $\text{Ca}^{2+}$  fluorescence was observed in the control cell group by confocal microscopy; (b)  $\text{Ca}^{2+}$  fluorescence in the siRNA-NC group showed similar intensity to the control group cells; (c) A considerable decrease in intensity of  $\text{Ca}^{2+}$  fluorescence was shown in siRNA group (Si); (d) Stronger intensity of  $\text{Ca}^{2+}$  fluorescence was detected in cells transfected with Frizzled-2 expression vector (FRI); (e) Quantitative analysis of the intensity of intracellular  $\text{Ca}^{2+}$  fluorescence among different groups. \* $p < 0.05$ , \*\* $p < 0.001$  vs. cell group; # $p < 0.05$ , ## $p < 0.001$  vs. Si group.

this study, we investigated the effects of Frizzled-2 signaling on autophagy activity under the H/R condition using rat hepatic BRL-3A cells (Figure 8). Our results revealed that H/R treatment induced Frizzled-2 expression and  $\text{Ca}^{2+}$  overload and reduced autophagy activity. The overexpression of Frizzled-2 impaired autophagy under normoxia by elevating the expression of Atg7 and Beclin-1 while suppressing the conversion of LC3-I to LC3-II and inducing the Caspase-3-dependent cell apoptosis (Figure 8a). In contrast, Frizzled-2 siRNA considerably induced autophagy activity in BRL-3A cells while it inhibited the intracellular  $\text{Ca}^{2+}$  level as well as apoptosis in BRL-3A, thereby attenuating the H/R-induced hepatic cell injury (Figure 8b). Our findings suggest that the suppression of the Frizzled-2/Wnt5a pathway partially protects liver cells from H/R injury via autophagy activation.

To address the potential hepatocyte functionality in response to HIRI, an *in vitro* H/R hepatic cell model was established by the incubation of rat normal liver BRL-3A cells under hypoxia (0.1% oxygen) for 4 h, followed by reoxygenation for 1 h (11), which can mimic *in vivo* hepatic cells under the HIRI condition and allow for *in vitro*

cellular functional and mechanistic studies. Our previous studies demonstrated that H/R treatment induces the expression of Frizzled-2 and Wnt5a, the level of intracellular  $\text{Ca}^{2+}$ , and cell cytotoxicity and apoptosis in BRL-3A cells. This induction was, in turn, attenuated by Frizzled-2 siRNA (11). These observations suggest that Frizzled-2/Wnt5a signaling mediates the H/R-induced intracellular  $\text{Ca}^{2+}$  level and cell injury in BRL-3A cells and that Frizzled-2 siRNA may have the potential to protect hepatic cells from the H/R challenge.

Autophagy is a dynamic process in which many molecular pathways participate in cellular proliferation, apoptosis, or cellular stress or injury. Other studies have shown that the induction of autophagy protects cells against HIRI (18, 19). Autophagy plays distinct roles in cells exposed to H/R. In this study, H/R treatment suppressed autophagy, which was associated with cell death, as evidenced by the induced expression of autophagy-related proteins Atg7 and Beclin-1, as well as the inhibition of autophagic flux in BRL-3A cells. The level of LC3B-I was upregulated by the overexpressed Frizzled-2 gene, whereas the transfection of Frizzled-3 siRNA induced the LC3B-II expression and



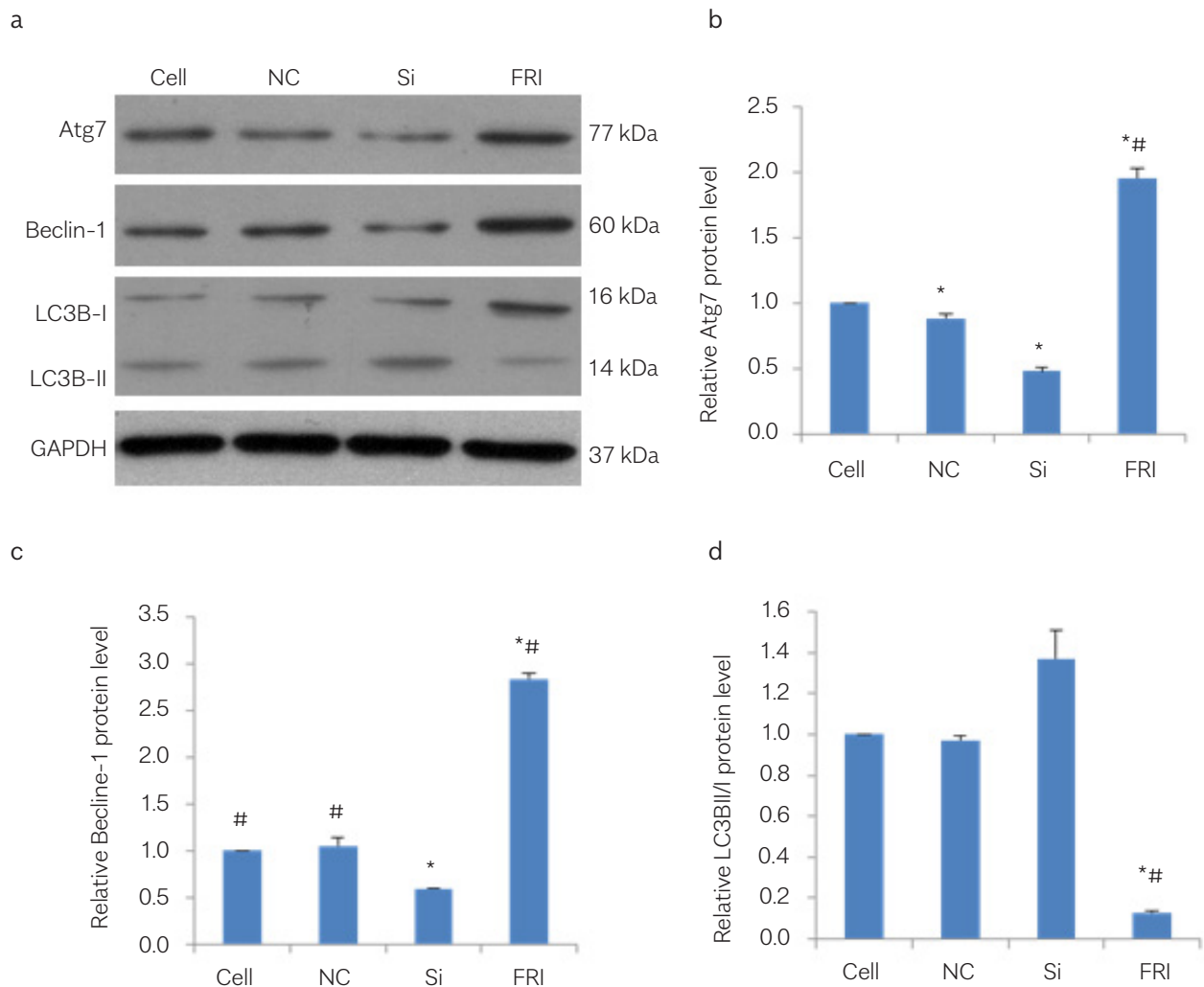


**Figure 5. a-d.** Effect of Frizzled-2 on the expression of autophagy-related proteins in BRL-3A cells. (a) Representative photographs of protein expression of Atg7, Beclin-1, LC3B-I/II, and GAPDH by immunoblotting; (b) Relative Atg7 protein expression; (c) Relative Beclin-1 expression; (d) The ratio of relative LC3B-I/II protein level. The band optical densities were measured to quantify the relative protein expression and normalize it to GAPDH. Bar graphs are presented as means $\pm$ SEM from three independent experiments. \* $p$ <0.05 and \*\* $p$ <0.001 vs. cell group, and # $p$ <0.05 and ## $p$ <0.001 vs. Si group.

LC3B-II/I ratio. It also attenuated the H/R-induced expression of Atg7 and Beclin-1, suggesting that cell autophagy activity was enhanced by Frizzled-2 siRNA, thereby mitigating cell injury and apoptosis in response to H/R treatment in BRL-3A cells. The increased autophagic flux in steatotic cells exposed to HIRI was correlated with a corresponding increase in cell death with an induced expression of several autophagy markers, such as LC3B-II, Atg7, beclin-1, HMGB1, and p62 (20). Beclin-1 plays a key role in regulating every major step in autophagic path-

ways from autophagosome formation to autophagosome maturation (21). The Beclin-1 expression was upregulated during cell stress but suppressed during the cell cycle (21). Autophagy under ischemia was accompanied by the upregulation of Beclin-1 expression in cultured cardiac myocytes during reperfusion. Autophagy and cardiac injury during the reperfusion phase were considerably attenuated by the inhibition of Beclin-1 expression (21). LC3B is a protein that is positively correlated with the induction of autophagy. The conversion of LC3B-I

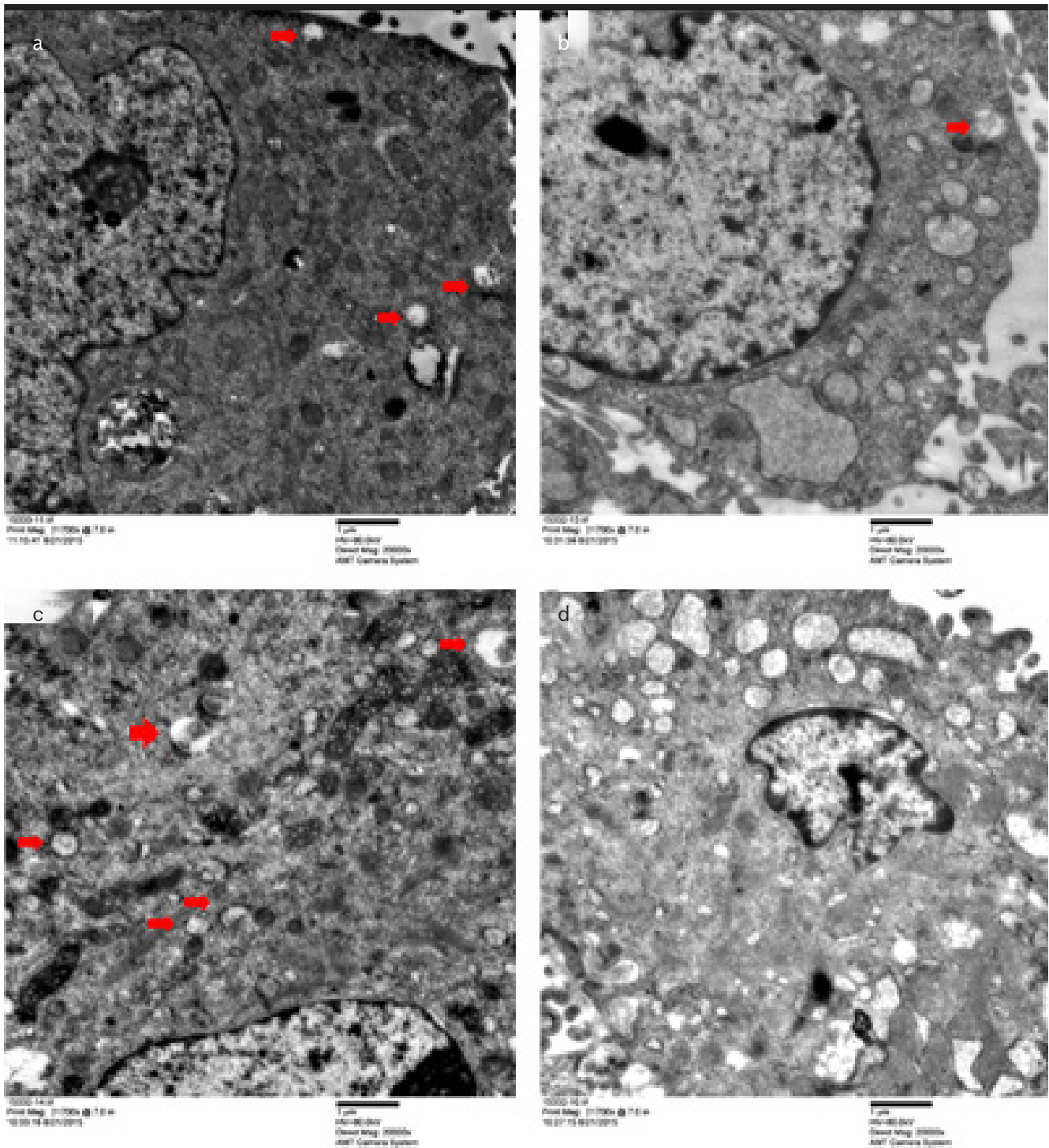


**Figure 6. a-d.** Frizzled-2 siRNA increased autophagosomes in BRL-3A cells. TEM scanning was performed in BRL-3A cells, with representative TEM images shown; (a) Cell group; (b) NC group; (c) Si group; (d) FRI group. The numbers of autophagosomes or autophagic vacuoles (red arrows) were determined. Scale bars denote 1  $\mu$ m.

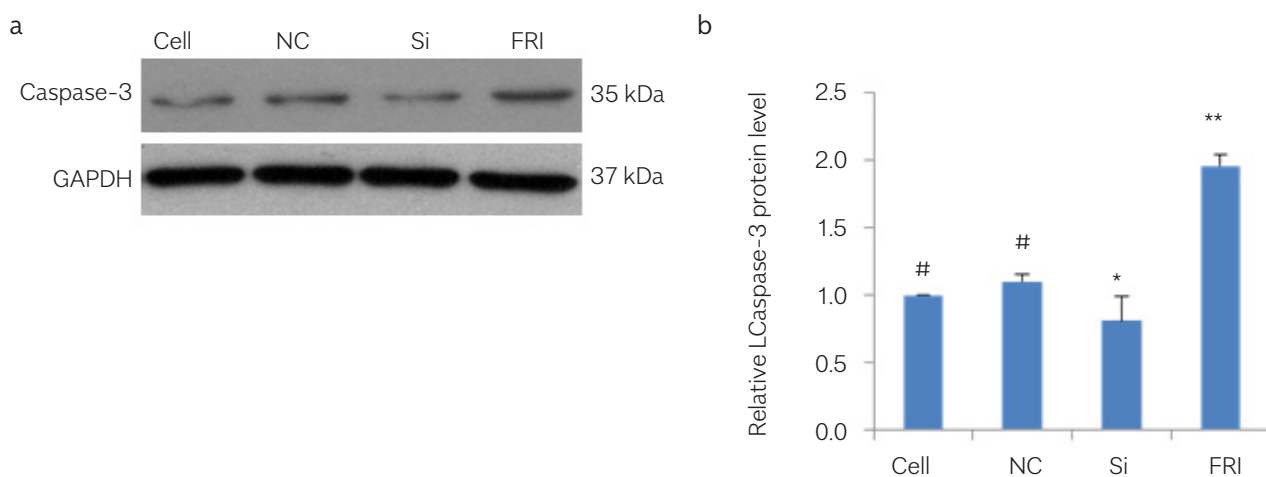


**Figure 7. a, b.** Frizzled-2 induced cell apoptosis in BRL-3A. (a) Representative photographs of protein expression of total Caspase-3 and GAPDH; (b) The band optical densities were measured to quantify relative total Caspase-3 protein level and normalize it to GAPDH. Data are presented as means $\pm$ SEM from three independent experiments. \* $p$ <0.05 when compared with cell group and # $p$ <0.05 when compared with the Si group.

to LC3B-II is the most common autophagosome marker because the amount of LC3B-II reflects the number of autophagosomes and autophagy-related structures. Another study showed that hypoxia and steatosis could be detrimental to autophagy (20). Our study demonstrated that Frizzled-2 siRNA suppressed the H/R-induced expression of autophagy-related proteins and recovered the H/R-impaired autophagy flux in BRL-3A cells. During the mimicking of H/R treatment, the overexpression of Frizzled-2 impaired autophagy under normoxia by elevating the expression of Atg7 and Beclin-1 while suppressing the autophagic flux by inhibiting the LC3-II to LC3-I ratio. A detailed study is needed to explore whether the H/R treatment modulation of autophagy is directly mediated by Frizzled-2/Wnt5 signaling.

Intracellular  $Ca^{2+}$  overload is one of the major pathological changes of ischemic tissue injury, which directly triggers cell death. Therefore, the control of intracellular  $Ca^{2+}$  concentration is critical in the treatment of ischemic injury (22). Our previous study showed that the Wnt5a/Frizzled-2 pathway has a critical role in controlling  $Ca^{2+}$  overload (11).  $Ca^{2+}$  concentration is a key determinant of ischemia-reperfusion-induced apoptosis (22). The  $Ca^{2+}$ -dependent pathway was involved in autophagy induction for notochordal cells under hyperosmotic stress (23). In this study, Frizzled-2 siRNA decreased the accumulation of  $Ca^{2+}$  while it increased the number of autophagosomes after H/R treatment, suggesting that Friz-

zed-2 siRNA induction of autophagy is intracellular  $Ca^{2+}$  dependent.

Caspase-3, a crucial mediator of cell apoptosis, is frequently activated to catalyze the specific cleavage of many key cellular proteins involved in the apoptotic cell death (24). The cross-regulation of autophagy and apoptosis may be involved in the H/R context through modulating the expressions of autophagy-related proteins and caspases (25, 26). In this study, the overexpression of Frizzled-2 induced cell apoptosis with an increased level of total Caspase-3 expression, which correlated with a corresponding decrease in the activity of autophagy. Nonetheless, more studies are needed to emphasize autophagy's contribution to apoptotic cell death in protecting the liver from HIRI.

The transfection of Frizzled-2 siRNA in BRL-3A cells mainly revealed the role of Frizzled-2. The main disadvantages of using siRNA transfection are a short half-life and a limited knockdown efficiency arising from a difficult delivery. The findings of this study using the *in vitro* cell lines should be further validated in the primary hepatocytes or *in vivo* animal studies.

Cell autophagy enables the cellular physiological response to stress or injury and promotes cell survival. A complex interplay between hepatic autophagy and apoptosis determines the fate of a cell during H/R-induced

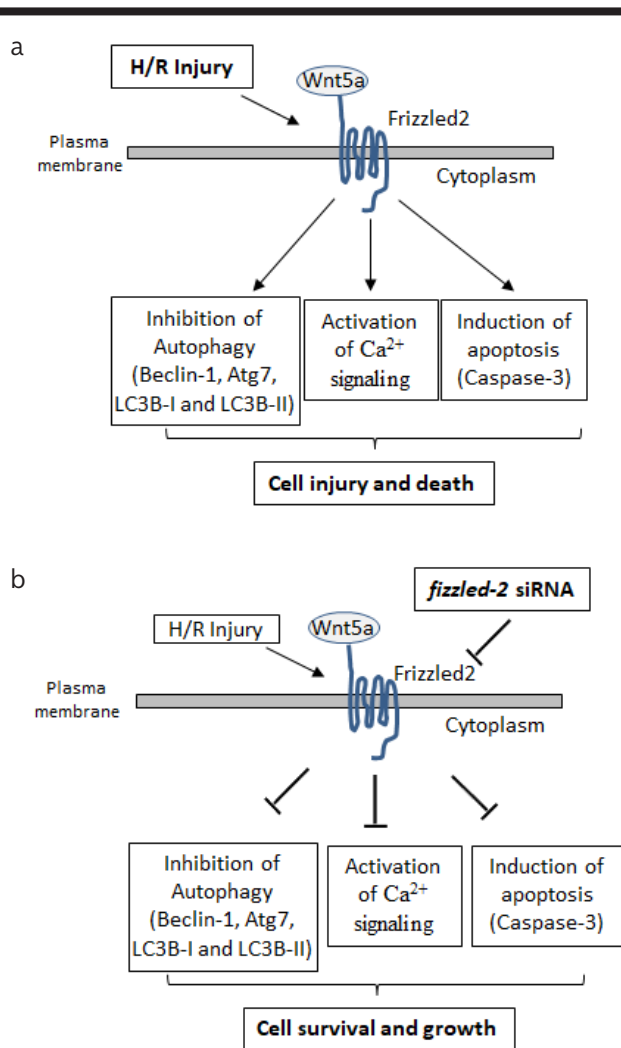


**Figure 8. a, b.** Frizzled-2 siRNA attenuates the H/R-induced hepatic injury in BRL-3A cells. (a) Mimicking H/R injury, Frizzled-2 overexpression inhibited hepatic autophagy activity. However, it increased intracellular  $Ca^{2+}$  accumulation and induced Caspase-3-dependent apoptosis, leading to cell injury and death. (b) Frizzled-2 siRNA protects hepatic cells by attenuating H/R-induced hepatic injury.

injury in BRL-3A cells. In this study, the overexpression of Frizzled-2 while mimicking H/R injury undermined the cellular autophagy activity but induced the cellular  $Ca^{2+}$  level and stimulated the Caspase-3-dependent apoptosis. Our results suggest that Frizzled-2 siRNA stimulates autophagy to protect hepatic cells by partially attenuating H/R-induced hepatic injury. Much more work is needed to further clarify the roles of autophagy in the pathophysiology of the liver and the signaling pathways involved in the regulation of autophagy and apoptosis in response to H/R injury.

In conclusion, H/R treatment induced Frizzled-2 expression and  $Ca^{2+}$  overload and reduced autophagy activity. The overexpression of Frizzled-2 impaired autophagy under normoxia by elevating the expression of Atg7 and Beclin-1 while suppressing the conversion of LC3-I to LC3-II and inducing cell apoptosis. Frizzled-2 siRNA partially protected BRL-3A cells from H/R treatment by enhancing autophagy activity. Thus, our findings suggest that silencing Frizzled-2 expression may be a potential therapeutic target for liver HIRI.

**Significance:** Our findings suggest that Frizzled-2 siRNA partially protects hepatic BRL-3A cells against H/R-induced hepatic injury via the activation of autophagy.

**Ethics Committee Approval:** Ethics committee approval was received for this study from the Ethics Committee of Zhujiang Hospital and Southern Medical University (No. ZJYY-2016-GDEK-001).

**Informed Consent:** NA.

**Peer-review:** Externally peer-reviewed.

**Author contributions:** Concept and Design – X.H., G.H., Y.G.; Supervision – Y.G.; Resource – Y.G.; Materials – Y.C.; Data Collection and/or Processing – X.H.; Analysis and/or Interpretation – C.Z.; Literature Search – X.H.; Writing – X.H.; Critical Reviews – M.P.

**Acknowledgements:** We thank Dr. David Fu for assisting in the preparation of this manuscript.

**Conflict of Interest:** The authors have no conflict of interest to declare.

**Financial Disclosure:** This research was supported by the Science and Technology Planning Project of Guangdong Province (2015B020229002), the National Natural Science Foundation of China (81470875) and the Natural Science Foundation of Guangdong Province (2014A030312013).

## REFERENCES

- Li C, Jackson RM. Reactive species mechanisms of cellular hypoxia-reoxygenation injury. *Am J Physiol Cell Physiol* 2002; 282: C22741. [\[CrossRef\]](#)
- Bhogal RH, Curbishley SM, Weston CJ, Adams DH, Afford SC. Reactive oxygen species mediate human hepatocyte injury during hypoxia/reoxygenation. *Liver Transpl* 2010; 16: 1303-13. [\[CrossRef\]](#)
- Zhai Y, Petrowsky H, Hong JC, Busuttil RW, Kupiec-Weglinski JW. Ischaemia-reperfusion injury in liver transplantation--from bench to bedside. *Nat Rev Gastroenterol Hepatol* 2013; 10: 79-89. [\[CrossRef\]](#)
- Teoh NC, Farrell GC. Hepatic ischemia reperfusion injury: pathogenic mechanisms and basis for hepatoprotection. *J Gastroenterol Hepatol* 2003; 18: 891-902. [\[CrossRef\]](#)
- Toffoli S, Michiels C. Intermittent hypoxia is a key regulator of cancer cell and endothelial cell interplay in tumours. *FEBS J* 2008; 275: 2991-3002. [\[CrossRef\]](#)
- Todde V, Veenhuis M, van der Klei IJ. Autophagy: principles and significance in health and disease. *Biochim Biophys Acta* 2009; 1792: 3-13. [\[CrossRef\]](#)

7. Bhogal RH, Weston CJ, Curbishley SM, Adams DH, Afford SC. Autophagy: a cyto-protective mechanism which prevents primary human hepatocyte apoptosis during oxidative stress. *Autophagy* 2012; 8: 545-58. [\[CrossRef\]](#)
8. Levine B, Mizushima N, Virgin HW. Autophagy in immunity and inflammation. *Nature* 2011; 469: 323-35. [\[CrossRef\]](#)
9. Klionsky DJ, Abdalla FC, Abeliovich H, et al. Guidelines for the use and interpretation of assays for monitoring autophagy. *Autophagy* 2012; 8: 445-544. [\[CrossRef\]](#)
10. Hoyer-Hansen M, Bastholm L, Szyniarowski P, et al. Control of macroautophagy by calcium, calmodulin-dependent kinase kinase-beta, and Bcl-2. *Mol Cell* 2007; 25: 193-205. [\[CrossRef\]](#)
11. Hu X, Zhou C, He G, Cheng Y, Pan M, Gao Y. Inhibition of Frizzled-2 by small interfering RNA protects rat hepatic BRL-3A cells against cytotoxicity and apoptosis induced by Hypoxia/Reoxygenation. *Gastroenterol Hepatol*. 2020 Jan 18. doi: 10.1016/j.gastrohep.2019.02.006. [Epub ahead of print] [\[CrossRef\]](#)
12. Petanceska S, Zikherman J, Fricker LD, Devi L. Processing of prodynorphin in BRL-3A cells, a rat liver-derived cell line: implications for the specificity of neuropeptide-processing enzymes. *Mol Cell Endocrinol* 1993; 94: 37-45. [\[CrossRef\]](#)
13. Eskelinen EL, Reggiori F, Baba M, Kovacs AL, Seglen PO. Seeing is believing: the impact of electron microscopy on autophagy research. *Autophagy* 2011; 7: 935-56. [\[CrossRef\]](#)
14. Glick D, Barth S, Macleod KF. Autophagy: cellular and molecular mechanisms. *J Pathol* 2010; 221: 3-12. [\[CrossRef\]](#)
15. Yun N, Cho HI, Lee SM. Impaired autophagy contributes to hepatocellular damage during ischemia/reperfusion: heme oxygenase-1 as a possible regulator. *Free Radic Biol Med* 2014; 68: 168-177. [\[CrossRef\]](#)
16. Rautou PE, Mansouri A, Lebrec D, Durand F, Valla D, Moreau R. Autophagy in liver diseases. *J Hepatol* 2010; 53: 1123-34. [\[CrossRef\]](#)
17. Gracia-Sancho J, Guixé-Muntet S. The many-faced role of autophagy in liver diseases. *J Hepatol* 2018; 68: 593-4. [\[CrossRef\]](#)
18. Kim JS, Nitta T, Mohuczy D, et al. Impaired autophagy: A mechanism of mitochondrial dysfunction in anoxic rat hepatocytes. *Hepatology* 2008; 47: 1725-36. [\[CrossRef\]](#)
19. Cardinal J, Pan P, Tsung A. Protective role of cisplatin in ischemic liver injury through induction of autophagy. *Autophagy* 2009; 5: 1211-2. [\[CrossRef\]](#)
20. Gupta NA, Kolachala VL, Jiang R, et al. Mitigation of autophagy ameliorates hepatocellular damage following ischemia-reperfusion injury in murine steatotic liver. *Am J Physiol Gastrointest Liver Physiol* 2014; 307: G1088-99. [\[CrossRef\]](#)
21. Kang R, Zeh HJ, Lotze MT, Tang D. The Beclin 1 network regulates autophagy and apoptosis. *Cell Death Differ* 2011; 18: 571-80. [\[CrossRef\]](#)
22. Chattopadhyay P, Chaudhury P, Wahi AK. Ca<sup>2+</sup> concentrations are key determinants of ischemia-reperfusion-induced apoptosis: significance for the molecular mechanism of Bcl-2 action. *Appl Biochem Biotechnol* 2010; 160: 1968-77. [\[CrossRef\]](#)
23. Jiang LB, Cao L, Yin XF, et al. Activation of autophagy via Ca(2+)-dependent AMPK/mTOR pathway in rat notochordal cells is a cellular adaptation under hyperosmotic stress. *Cell Cycle* 2015; 14: 867-79. [\[CrossRef\]](#)
24. Porter AG, Janicke RU. Emerging roles of caspase-3 in apoptosis. *Cell Death Differ* 1999; 6: 99-104. [\[CrossRef\]](#)
25. Tsapras P, Nezis IP. Caspase involvement in autophagy. *Cell Death Differ* 2017; 24: 1369-79. [\[CrossRef\]](#)
26. Sun Q, Gao W, Loughran P, et al. Caspase 1 activation is protective against hepatocyte cell death by up-regulating beclin 1 protein and mitochondrial autophagy in the setting of redox stress. *J Biol Chem* 2013; 288: 15947-58. [\[CrossRef\]](#)